

Internet of Biomedical Things (IoBT)

The IoBT, also referred to as Internet of Bodies, broadly pertains to wearable, implantable, ingestible, and injectable IoT devices which can be used for a broad scope of applications such as medicine, wellness, sport/fitness, entertainment, to name but a few [1]. Having its root in wireless body area networks (WBANs) [353], the IoBT is an imminent extension to the vast IoT domain and has been recognized as a critical technology for revolutionizing the public health and safety sector, which has been proven to be inadequate during the humanitarian and economic crisis caused by the novel coronavirus pandemic (a.k.a, COVID-19) [354]. IoBT differs from their indoor/outdoor IoTT counterparts because of the distinctive QoS/Quality of Experience (QoE) demands of medical applications as well as peculiar and dynamic channel impairments in-on-and-around the human body. In particular, IoBT designed for patient monitoring applications has stringent reliability, latency, and security requirements as it handles users' critical and sensitive physiological data. However, miniaturization efforts to improve QoE of implantable, ingestible, and injectable IoBT devices leave a limited room for the battery size. Therefore, limited energy availability stands as the major obstacle in the way of fulfilling these multiple and conflicting QoS demands at the same time.

Accordingly, this section first provides a comparative analysis to provide valuable insights into how OWC can complement traditional RF-IoBT. Then, we present subtle issues related to in/on/off-body OWC-IoBT and survey the literature. Since operational lifetime is one of the primary design issues, SLIPT is also covered. Lastly, we conclude the section with a summary, insights, open problems, and future research directions.

A. A Comparative Analysis of RF-IoBT and OWC-IoBT

The RF channel attenuation dynamics in-on-and-around the human body are quite distinct from regular RF channels because of the lossy, heterogeneous, and dielectric nature of the human body. Different tissue types exhibit various propagation phenomena (e.g., reflection, refraction, diffraction, absorption, scattering) at different frequencies with varying levels. In-body channel gains are primarily determined by the distance between the transceivers as well as dielectric properties of tissues and organs along the propagation path. On the other hand, placement of on/off-body RF-IoBT directly determines the link distance and type (LoS or NLoS) as a result of irregular body shapes and curvatures. These factors have a significant impact on the first-order channel statistics (FoCS), i.e., path loss and shadowing. Unlike the in-body RF-IoBT devices, on/off-body RF-IoBT devices are also susceptible to the dynamic changes in the body postures/gaits and surrounding environment. Therefore, both intentional and involuntary mobility of the human body yield time-variant changes in path loss and shadowing effects, which determines the second-order channel statistics (SoCS) such as delay spread, power delay profile, level crossing rate, average fade duration, autocorrelation) channel statistics. Since FoCS/SoCS follow different distributions at different frequency bands and channel mediums (air, skin, deep tissue), the IEEE 802.15.6 standard specified a wide variety of narrowband (NB) and ultra-wideband (UWB) channels for the use of WBANs [355]. Next, we provide a comparative analysis between NB/UWB RF-IoBT and OWC-IoBT from different aspects:

- The radio front end is one of the most complex and power-hungry sub-systems of RF-IoBT devices. Hence, it limits the operational lifetime per charging cycle and necessitates a larger battery capacity. This naturally requires a larger packaging and frequent replacement, which is not a viable option, especially for implantable, ingestible, and injectable IoBT. Alternatively, OWC-IoBT transceivers can have package size in millimeter-scale thanks to available pico LEDs with less than 1 mm³ and PD arrays of several mm² area. Moreover, recent advances in LED fabrication has made it possible to have wall-plug efficiency more than unity. For example, authors of [356] reported 69 pW of light using 30 pW of supplied electrical power. By also using simple light modulation schemes, miniature and energy-efficient OWC-IoBT can provide very high bit/joule levels for long-life yet high-performance IoBT devices desired by many applications.
- RF-IoBT modules are susceptible to interference and co-existence issues with the nearby IoT devices operating on the same band, which exacerbates in crowded license-free RF bands. For example, IoT devices are typically designed to operate on ISM bands for two reasons: 1) there is no associated licensing fee, and 2) the ISM compatible RF front end modules are cheap and readily available. Considering the ever-increasing number of IoT devices, interference and co-existence problems are non-trivial for IoBT applications that require URLLC. Noting that light spectrum is also license-free, interference and co-existence issues for OWC-IoBT is minimal thanks to the vast spectrum availability, high directivity, and low penetration attributes of lightwaves. Even though on/off-body OWC-IoBT transceivers operating at VL spectrum are susceptible to ambient light sources, NIR transceivers are preferable by in/on/off-body OWC-IoBT thanks to their innate immunity to ambient light as well as favorable channel gains inside the body.
- As a result of highly radiative and omnidirectional RF propagation, RF-IoBT inadvertently permits eavesdroppers to intercept or even alter the original data. Thus, it is crucial to guard confidentiality and privacy of sensitive physiological information against eavesdropping, overheard, and cyber-attacks. However, adding extra security measures increases both hardware complexity and monetary cost, negatively impacting the miniature, low-cost, and ultra-low-power design goals. Alternatively, high directivity and low penetration features of lightwaves also provide inherent PHY layer security.
- Exposing the body to excessive electromagnetic radiation causes tissue burnt due to the increasing heat, raises the likelihood of developing cancer and body rejection of the implanted/injected devices. In fact, the International Agency of Research on Cancer (IARC) evaluation report in 2011 concluded that RF waves can possibly increase the risk of human brain tumors [357]. Therefore, RF-IoBT devices are subject to stringent specific absorption rate constraints, which stands as a main delimiter of the overall communication performance. Alternatively, the human safety regulations are relatively more lenient for the light emission since a very limited electrical energy transferred to heat thanks to the aforementioned high wall-plug efficiency.

The IEEE 802.15.6 has also defined body channel communication (BCC), a.k.a. intrabody communication, as a third PHY layer option, where transmission is confined to the human body by coupling electrostatic or magnetostatic signals to the skin through electrodes [18], [358], [359], [360], [361]. In addition to being more energy-efficient than RF-IoBT, the BCC also has relatively better PHY layer security due to less signal leakage. However, the BCC can merely be used for on-body IoBT devices and may not provide very high throughput as it is limited to 10 kHz-100 MHz band. Albeit its inherent virtues described above, OWC-IoBT should not be considered as a competitor or replacement technology of the RF-IoBT. For example, OWC-IoBT can be quite attractive solution for on/off-body applications. However, its functionality for the in-body applications are limited to transdermal telemetry as the penetration depth of lightwaves are very limited for deep tissue communications. In what follows, we discuss where and how OWC-IoBT can complement RF-IoBT devices in detail.

B. On-Body and Off-Body OWC-IoBT

As shown in Fig. 12, on-body OWC-IoBT devices can inter-communicate in three ways: 1) on-body LoS links, 2) on-body NLoS links through a nearby reflecting surface, and 3) traversing an AP by means of off-body LoS/NLoS links. However, due to the aforementioned dynamic channel conditions on and around the human body, regular indoor OWC channel models used by indoor OWC-IoTT devices are not directly applicable to these three cases. One can observe from Fig. 12 that on-body links can be realized by a time-variant combination of the first and second case since having LoS links may not always be possible as a result of node orientation and deployment on the body. A comprehensive study on channel characterization and modeling for on/off-body OWC channels has recently investigated FoCS and SoCS by considering both body-part movement (local mobility) and whole-body movement (global mobility) [380].

Although it has been shown that node placement and orientation along with the body geometry have a significant impact on channel statistics, the overall channel gain was observed to be frequency non-selective, and ISI was negligible. Unlike 0.2-4 dB attenuation changes caused by the local mobility, the global mobility was the primary determinant of the high attenuation and random variations. Moreover, Gamma distributions were found to provide the best Akaike-Information criteria fit models for the channel attenuation. On the other hand, time-variations were shown to change with node locations on the body and overall smaller than its RF counterparts. In what follows, we present major research efforts on on/off-body OWC-IoBT, which are categorized based on research type (e.g., implementation, simulation) and tabulated in Table VII.

TABLE VII The Major OWC-IoBT Studies Based on Node Locations

| IoBT Type | Study Type | Ref. | Year | Application | IoT MWL | Band | OWC | | | | | | Comp. Tech. | Higher Layers |
|--|----------------|-------|------|-------------|---------|---------|-----------|---------|---------|-----------|----------|-------|-------------|---------------|
| | | | | | | | Topology | Tx Type | Rx Type | Data Rate | Distance | Mod. | | |
| On-Body & Off-Body | Implementation | [362] | 2017 | EEG | N/A | VL | Broadcast | LED | OC | 2.4 K | 4.5 m | OOK | N/A | N/A |
| | | [95] | 2017 | ECG | Custom | VL | Broadcast | LED | PD | 40 K | 8 m | OOK | RF | N/A |
| | | [108] | 2019 | e-Health | N/A | NIR | Broadcast | LED | PD | 6.4 M | 1.5 m | OOK | N/A | N/A |
| | | [363] | 2019 | e-Health | N/A | VL | Broadcast | LED | OC | 1 K | 1 m | N/A | N/A | N/A |
| | | [364] | 2015 | e-Health | N/A | NIR | Star | LED | PD | 118 K | 5-7 m | OOK | N/A | OCDMA |
| | Simulation | [365] | 2015 | e-Health | N/A | NIR | Star | LED | PD | <1 M | 5-7 m | OOK | N/A | N/A |
| | | [366] | 2017 | e-Health | N/A | VL | Broadcast | LED | PD | N/A | N/A | OOK | N/A | N/A |
| | | [367] | 2019 | ECG | N/A | VL | Broadcast | LED | OC | N/A | 4 m | N/A | BLE | N/A |
| | | [368] | 1992 | VAD | N/A | NIR | P2P | LED | PD | 9.6 K | 15 mm | FSK | N/A | N/A |
| | | [369] | 2001 | SLIPT | N/A | IR | P2P | L(E)D | PD | 1 M | 10 mm | Phase | N/A | N/A |
| In-Body IoBT (Transdermal OWC) | Implementation | [370] | 2004 | NPT | N/A | NIR | P2P | LED | PD | 40 M | 4 mm | AM | RF | N/A |
| | | [371] | 2004 | e-Health | N/A | NIR | P2P | LED | PD | 1 M | 24 mm | IrDA | N/A | N/A |
| | | [372] | 2005 | VAD | N/A | NIR | P2P | LED | PD | 9.6 K | 45 mm | ASK | N/A | N/A |
| | | [373] | 2008 | NPT | N/A | NIR | P2P | LD | PD | 16 M | 2-8 mm | N/A | N/A | N/A |
| | | [374] | 2012 | AMI | N/A | NIR, VL | P2P, RR | L(E)D | PD | N/A | 1 mm | OOK | N/A | N/A |
| | | [375] | 2012 | NPT | N/A | NIR | P2P | VCSEL | PD | 50 M | 2-6 mm | OOK | N/A | N/A |
| | | [375] | 2014 | NPT | N/A | NIR | P2P | VCSEL | PD | 75 M | 2-6 mm | OOK | N/A | N/A |
| | | [376] | 2014 | NPT | N/A | NIR | P2P | VCSEL | PD | 100 M | 2-6 mm | OOK | N/A | N/A |
| | | [377] | 2015 | BCI | N/A | NIR | P2P-UL | VCSEL | PD | 100 M | 2 mm | OOK | N/A | WDM |
| | | [378] | 2017 | BCI | N/A | NIR | P2P-DL | VCSEL | PD | 1 M | 0.2 mm | PWM | N/A | N/A |
| | | [379] | 2020 | ECG | N/A | IR | P2P | LED | PD | 4 K | 4-16 mm | UPIM | N/A | UART |
| Legend: BCI: Brain Computer Interface, NPT: neuroprosthetic telemetry, VAD: ventricular assistance device, L(E)D: LED & LD, K: Kbps, M: Mbps | | | | | | | | | | | | | | |

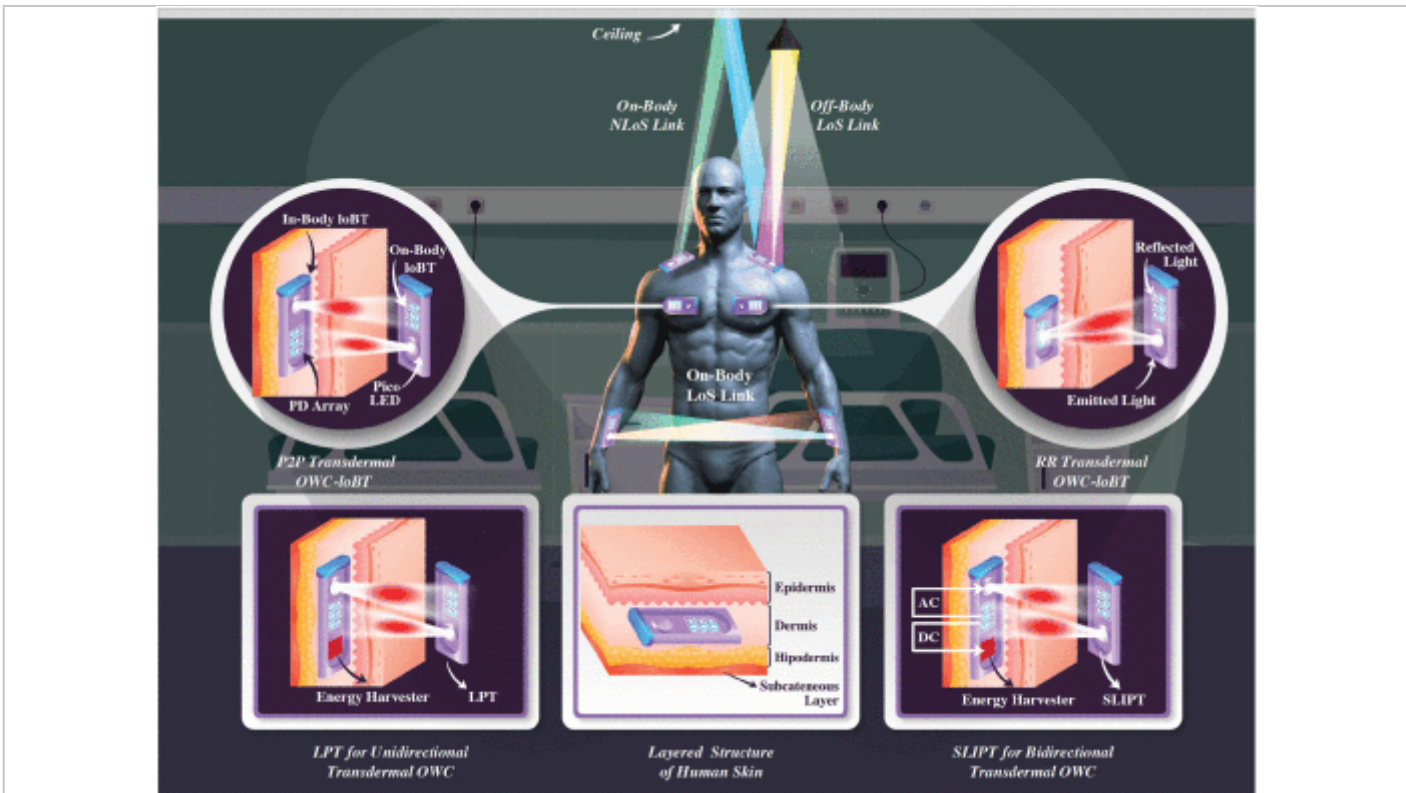


Fig. 12.

Illustration of LoS, NLoS, and RR link configurations for in/on/off-body OWC-IoBT.

Show All

In [362], Rachim et al. created an experimental LED/OCC setup for transmitting electroencephalogram (EEG) data. This study used a single white LED to transmit over LoS to a smartphone located on a tripod stand within the same room. By consuming 3 W power, they achieved an error-free transmission with an upload speed of 2.4 Kbps at a distance of 4 meters. They claimed that this type of data transfer may replace common RF protocols used by wearable devices as a physiologically safer alternative. Even though the authors discussed no application protocol, the transmitted EEG data could be wrapped in an IoT application protocol to enable aggregation and automated healthcare monitoring to further improve its utility in IoT.

In another implementation by An et al., an LED/PD link was used to transmit data from multiple ECGs to a custom made dashboard for cardiac health monitoring of patients [95]. By using lenses with the LEDs, the authors were able to send data at 40 Kbps at a distance of 8 m. This implementation explored time hopping as a way to send multiple signals to the same PD receiver. The authors also considered using RF technology to supplement the link when the LoS link is broken.

Dhatchayeny et al. expanded their previous work in [366] and offered a new use case in [108] for biomedical sensors to transmit via IR-LED to reduce crowding of the RF spectrum within hospitals and allow high data rate transmission in RF sensitive environments. They implemented an LED/PD link to transmit patient's biomedical data from multiple health sensors to a single overhead receiver, which allows multiple patients to be monitored in the same room by using a transmission scheduling scheme. An IR-LED choice means that there is no VL to disturb patients or health-care providers, but retains high data rate and secure LoS communications while not causing RF interference. The real-time information can be monitored by a server and send alerts to providers when coupled with an IoT application protocol. The experimental setup enabled transmission at 1.5 m at 6.4 Mbps, but no IoT Network layer application protocol was tested in the research.

The same authors also propose an experimental LED/OCC link in [363] that can be used to transmit vital sign data. The main consideration was that the link would have a lower BER to ensure that critical health data remains accurate over the link. The setup involved a 4×4 panel of RGB LEDs to transmit 48 bits per frame and a 30 fps rolling shutter camera. The experimental setup demonstrated a low BER value transmission of 1.2×10^{-4} with a rate of 960 bps at a distance of 1 m. The transmissions were directly translated into vital sign data, but an application protocol could be utilized over such a link to enable data aggregation.

In [364], Chevalier et al. investigated the BER performance of a star OWC-IoBT network topology. Theoretical analyses are validated by a simulation set up where a patient is moving in a hospital room. Since they consider multiple nodes randomly located on the patient's body, they exploit optical code division multiple access (OCDMA) to avoid MAI among the nodes. In [365], the same authors provide outage performance analysis for NLoS communications based on a similar simulation setup. They developed a fast, simple, and adaptive method to consider mobility and the presence of obstacles within an indoor environment.

In [366], Dhatchayeny et al. simulated an LED/PD link that sent vital sign measurements to a gateway. The simulation did not mention BER or distances but instead focused on SNR versus BER. The team found that they were able to transmit four different signals to the same receiver with a minimal BER when the SNR value is around 12 dB, which shows that the MIMO healthcare data aggregation is reliable under the considered conditions.

In [367], Hasan et al. simulated a hybrid OWC/RF link system to improve the reliability of the signal from healthcare devices while lowering the amount of RF transmission. The OWC link simulated is an LED/OCC link, and the main component studied was the

reliability of the link. When the OCC link becomes unreliable, the RF channel was utilized instead. The authors found that increasing the number of cameras in the room decreased the need to switch to the RF channel and that the OCC link was viable up to 4 meters.

C. Transdermal OWC for In-Body IoBT

The injected and implanted in-body IoBT devices can be at depths from a few millimeters to a few centimeters. In comparison with its on/off-body counterparts, in-body IoBT has more stringent contradictory design requirements such as small form-factor for users' comfort and long battery life, which requires ultra-low-power consumption at μW levels. As shown in [Fig. 12](#), the in-body OWC-IoBT devices can communicate with on-body devices through P2P or RR transdermal (a.k.a., transcutaneous) OWC links. Unfortunately, among many other tissue types, the skin has the most complex structure and the highest absorbing losses due to its layered and relatively low-water content. As shown in [Fig. 12](#), the skin tissue consists of four main layers: epidermis, dermis, hypodermis, and transcutaneous layer. Fortunately, lightwaves within a specific wavelength range can penetrate the skin with significantly low absorption losses. The absorption losses [dB/mm] of various tissue types at different wavelengths are shown in [Fig. 13](#) where a favorable channel gain window can be observed through the end (600-750 nm) and at the beginning (750-900 nm) of VL and NIR spectrum, respectively. Since commercial LEDs are readily available at these wavelengths, there are considerable theoretical and experimental research efforts on both VL and NIR based transdermal OWC-IoBT. Although in-body OWC links experience a much higher path loss compared to over the air on/off-body OWC links, they are more stable and reliable due to their isolation from body mobility and environmental changes. In what follows, we present major research efforts on transdermal OWC for in-body IoBT, which are also tabulated in [Table VII](#). The main applications of transdermal OWC can be exemplified as various implants (e.g., cochlear, retinal, cortical, foot drop, etc.), the gastric stimulators, the wireless capsule endoscope, the insulin pumps, and the implantable orthopedic devices [\[382\]](#).

The earliest example of an LED/PD OWC link in IoT is the work presented by Miller et al. [\[368\]](#). In this work, IR-LEDs are utilized to transmit data to and from a ventricular assistance device (VAD) through an implanted PD. The application is capable of maintaining an error-free link of 9600 bps at 150 mm. This paper's main focus is to have the LED/PD transceiver implanted in the patient to allow a wireless link with the VAD. Using an LED/PD link Abita and Schneider created a link that sent data through porcine skin samples at 1 Mbps [\[371\]](#). They used an IR-LED and PD transceiver to send and receive data with an Active Medical Implant (AMI) at a distance of 24 mm. The AMI can be used in many different situations and can allow care providers to receive patient health information after the AMI is implanted quickly. The authors did not discuss higher-level applications, such as aggregating patient data over time. However, the AMI devices used were capable of storing up to 512 Kbps so that longer-term data could be given to the care provider or wearer regularly. Another example of transcutaneous LED/PD communication was found in [\[372\]](#), where Okamoto et al. tested both IR and VL LEDs. They found that both IR and VL were able to transmit unhindered at 9600 bps, but the IR-LED transmitted without error at a distance of 45 mm while the VL-LED was capable of transmitting error-free up to 20 mm.

In [370], Guillory et al. developed a hybrid RF/IR neuroprosthetic telemetry (NPT) system that uses constant-frequency RF inductive links for energy and amplitude modulated transcutaneous IR signals for data transfer. Numerical results showed that with commercially available IR components, data rates of up to 40 Mbps can be transmitted through 5 mm skin with an internal device power dissipation under 100 mW and a BER of 10^{-14} . In [373], Parmentier et al. developed an IR-LD-based NPT system and evaluated its performance in various operating conditions. The system can transmit at data rates up to 16 Mbps through a skin thickness of 2–8 mm while achieving a BER of 10^{-9} with a consumption of 10 mW or less. In [374], Gil et al. explored the feasibility of P2P and RR transdermal OWC links through both mathematical models and experimental validations. The P2P and RR link measurements showed that an 800–950 nm wavelength window is desirable for transdermal OWC. Although authors did not specify achievable data rates, OOK modulation achieve a 10^{-5} BER over P2P and RR link by consuming 0.3 μ W and 4 mW transmission power, respectively. Since authors considered a 1 mm skin sample, the presented results could be optimistic for the AMI placed in deeper tissues.

In [375], Liu et al. develop an NPT system by using vertical-cavity surface-emitting lasers (VCSELs) in both transmitter and implanted receiver modules. For a power consumption less than 4.1 mW, the developed system is capable of achieving a 50 Mbps data rate through a 4 mm tissue with a BER less than 10^{-5} and a tolerance of 2 mm misalignment. In [383], authors improved the system throughput up to 75 Mbps by consuming 2.8 mW, which is almost half of the reported value in [375]. In [376], by conducting an in-vivo test on a sheepskin, authors further improved the data rates up to 100 Mbps with a BER of 2×10^{-7} while limiting the power consumption to 2.1 mW. In [377], Liu et al. also developed a bi-directional brain-computer interface (BCI) using transdermal OWC links by utilizing a VL-VCSEL and NIR-VCSEL in downlink and uplink directions, respectively. In-vitro experiments on a 2 mm porcine skin showed that the developed OWC-BCI system could achieve 1 and 100 Mbps rates in downlink and uplink directions by consuming 290 μ W and 3.2 mW, respectively.

In [378], Takehara et al. developed an injectable image sensor of size $400 \times 1200 \mu\text{m}^2$, which can modulate a small NIR-LED with PWM. The modulated signal was transmitted through a mouse skull bone of 200 μm thickness, which successfully received the 2700 pixel/frame image. Most recently, Sohn et al. developed an ultra-low-power AMI with a small form factor of $10 \times 10 \times 1 \text{ mm}^3$ in [379]. The authors developed an unsynchronized pulse-interval-modulation (UPIM) along with a new protocol to account for the sparse, low-rate, but delay-sensitive nature of transdermal OWC.

In the last couple of years, there is also a growing interest in theoretical transdermal OWC studies such as performance analysis and signal quality assessment in the presence of misalignment [384], [385], [385]; modeling and analysis of optical cochlear implants based on key performance indicators such as the probability of hearing and neural damage [386], [387]; and developing diversity techniques to improve outage performance in the presence of pointing errors for P2P links [388] and RR links [389], [390]. Although understanding the fundamental issues through

theoretical studies is important, we believe their true impact can be unleashed only if proposed models are validated by experimental setups.

D. SLIPT Towards Energy Self-Sustainable OWC-IoBT

In addition to the ultra-low-power design goal, in-body IoT also requires energy self-sustainability through energy harvesting techniques. The lightwave power transfer (LPT) has already been considered as an effective solution for wireless charging of body implants [391], [392], [393], [394], [395]. A generic LPT system is shown in Fig. 12 where an external light source emits a DC lightwave, which is received by a PD and fed into an energy harvester circuit. The harvested energy is then used for transmitting information to the external device. Therefore, the LPT is limited to unidirectional (i.e., uplink) transdermal OWC. The earliest example of LPT was presented in [391], where a 10×10 mm PD was charged by an IR-LD to empower a pacemaker that consumes about 2 mW. In [392], Moon et al. developed $1\text{--}10$ mm² silicon photovoltaic (PV) cells and achieved a power conversion efficiency of more than 17% for 660-nW/mm² illumination at 850 nm. They further extended this work in [393], where PV cells were able to harvest energy from both VL and IR resources in the range of 650–950 nm wavelengths. Although these prototypes show the feasibility of energy harvesting of implanted devices from external light sources, they do not consider the information and power transfer together.

For applications that require real-time and interactive communications with the in-body IoT devices, a more practical approach is realizing bidirectional transdermal OWC by means of SLIPT technology [396]. In the SLIPT [c.f. Fig. 12], the transmitted lightwave has both AC and DC components. At the receiver side, AC and DC components are split in parallel by using an inductor and a capacitor at the energy harvester and decoder branches, respectively [25]. Unlike its RF counterpart (i.e., simultaneous wireless information and power transfer), the SLIPT does not require switching between modes since the DC bias is always necessary for IM/DD. However, the literature on transdermal SLIPT is limited to [369], where Goto et al. extended their previous IR-LPT systems in [394], [395] to an IR-SLIPT system where two implanted PDs receive IR-LD irradiation. The carrier wave generated by the first PD is phase modulated and fed into the transmitter implanted NIR-LED, which is powered by the second PD. The size and the weight of the implanted OWC-IoBT were $14 \times 12 \times 4$ mm and 1.1 g, respectively.

E. Summary and Insights

The IoT devices are expected to play an important role in the post-COVID-19 world to make health-care more affordable and reachable for everyone. However, commercially available IoT devices mostly operate on RF bands and share common disadvantages such as i) limited operational lifetime due to complex and power-hungry radio front ends, ii) reliability and latency issues due to interference from co-existing devices on the same band, iii) vulnerability to security threats as a result of highly radiative nature of RF propagation, iv) and being restricted by stringent safety regulations on electromagnetic radiation in and on the human body. As noted above, OWC-IoBT devices can be a viable alternative since they are not affected from such drawbacks. Accordingly, this section provided a taxonomy of OWC-IoBT devices based on node locations and present theoretical, numerical, and experimental advances in various

aspects. The state-of-the-art is also tabulated in [Table VII](#) which categorizes literature based on study and application type, spectrum, topology, Tx/Rx types, achieved rates, link distance, modulation type, complementary technology, and protocols used in higher layers. Indeed, [Table VII](#) helped us to gain deep insights into the open research challenges and future research directions, which are discussed in detail below.

1) The Need for an IoBT Protocol Stack:

It is obvious from [Table VII](#) that most of the existing works merely focus on PHY aspects without accounting for its impacts on higher layer functionalities. Considering the ultra-low-power and URLCC requirements of IoBT applications, there is a dire need for a protocol stack that integrates OWC to higher layers. For example, the majority of works reported above employed OOK modulation for its simplicity at the expense of higher power consumption. Although commercial modules that follow IrDA standards employ return-to-zero modulation with shorter pulse duration, they still fail to satisfy μW power consumption levels. Alternatively, the pulse interval modulation (PIM) was shown to consume much less transmission power since it uses a single short pulse to encode a symbol while OOK roughly generates pulses as many as the 50% of the transmitted bits [\[379\]](#).

Even though some of the works in [Table VII](#) report very high data rates, these may not be practical for physiological data which is small in size but sensitive to delay by its nature. Therefore, more emphasis should be on tradeoff between throughput, BER, delay, and overall reliability. In this regard, Sohn et al. also developed an OWC protocol to address both energy efficiency and delay sensitivity based on asynchronous PIM. The experimental results on developed prototype showed that their cross-layer protocol can deliver a significantly lower power consumption ($392 \mu\text{W}$) than IrDA and Bluetooth Low Energy (BLE).

Another important but unexplored area is investigating effective and simple multiple access schemes. This is especially necessary for several on/off-body OWC-IoBT devices operating within the same environment. Excluding OCDMA in [\[364\]](#) and WDM in [\[377\]](#), existing implementations mostly deal with broadcast topology without paying attention on potential access schemes for MAI. We believe more comprehensive theoretical and experimental work is needed for the sake of standardization of PHY and MAC layer functionalities of OWC-IoBT.

2) Standardization and Commercialization Efforts:

Although IEEE 802.15.4 standard specifies PHY and MAC layer aspects of generic wireless personal area networks, it has been realized that it is not adequate to fulfill the requirements of WBAN. Therefore, the IEEE 802.15.6 standard has been developed as a PHY and MAC layer standard for ultra-low-power and secure communications and networking for RF-IoBT devices. Unfortunately, the IEEE 802.15.6 standard does not recognize OWC as one of its PHY techniques.

As discussed in [Section II](#), IEEE 802.15.7 has been developed to embrace many OWC technologies (VLC, IR, UV, OCC, etc.) by defining different device classes (infrastructure, mobile, vehicle) with five different PHY types for different QoS

requirements. Unfortunately, IEEE 802.15.7 does not recognize IoBT devices as well as their specific PHY and MAC layer distinctions. In its current form, it is similar to IEEE 802.15.4 and a new standard is needed for OWC-IoBT similar to IEEE 802.15.6. We believe an OWC-IoBT standard can be developed based on lessons learned from IEEE 802.15.6 and IEEE 802.15.7 standards. This new standard will eventually pave the way for commercialization of OWC-IoBT devices, which is mostly within the interest of academy.

3) Conflation of RR and SLIPT Concepts:

Even though the LPT is studied well in the literature, the potential of SLIPT concept for OWC-IoBT devices is waiting to be unleashed. Since the LPT is nothing but the foundation of the SLIPT, we believe there are many open research problems in developing prototypes and algorithms to coordinate energy harvesting and communications for energy self-sustainable OWC-IoBT devices. To the best of author's vision, conflation of RR communication and SLIPT is a promising and interesting direction. As shown in [Fig. 12](#), the RR-OWC consists of skin-surface light source and an implanted reflector. Similar to backscatter communication RF systems, the reflector modulates the continuous light beam emitted from the source and reflect it back to the receiver [\[374\]](#). Since the modulation power is negligible, the energy harvested by SLIPT would be sufficient to design energy self-sufficient design.